FAN NOISE ANALYSIS USING A MICROPHONE ARRAY

Olivier MINCK[1], Nicolas BINDER[2], Olivier CHERRIER[2], Lucille LAMOTTE[1], Valérie BUDINGER[2]

[1] *MicrodB, 28 chemin du Petit Bois, 69130 ECULLY, France*

[2] *ISAE, 10, avenue Edouard Belin - BP 54032. 31055 TOULOUSE, France*

SUMMARY

The purpose of this paper is to show the capabilities of MicrodB's acoustic imagery algorithm to characterize rotating sources. First part will explain the main specificity of the treatment. In the second part, possibilities of analysis and validations on simple tests will be demonstrated. In the last part, an industrial application will be studied : a Technofan extract fan with a 10000 RPM rotational speed will be analysed. Both fixed and rotating sources will be separated, allowing the localization of rotating sources on the blades.

INTRODUCTION

For many years now, acoustic arrays are successfully used for sound sources localization. Most of applications concern stationary sources with a fixed radiating surface. Fans present both, stationary and rotating sources, that make current algorithm non useable for localization. To properly study all rotating sources, MicrodB has developed an algorithm as part of its standard array software that takes into account the rotational characteristics of the sources. It allows the engineers to study industrial fans, and understand where the noise is generated.

BEAMFORMING FOR ROTATIVE SOURCES

Beamforming equations

For stationary sources, beamforming in temporal domain is basically given by the expression:

$$P(s,t) = \sum_{m=1}^{M} w_m P_m(t + \Delta_m(s)) \qquad (1)$$

with $P(s,t)$ the pressure estimation at the source location s, $\Delta_m(s)$ the time delay between the focused point s and microphone m, w_m the weighting applied on microphone m, and $P_m(t)$ the temporal signal recorded on microphone m.

For rotating sources, previous work [1] has demonstrated the capacity of temporal approach to easily locate sound sources. The beamformed signal is processed by calculating reception date for each position of the source (figure .1).

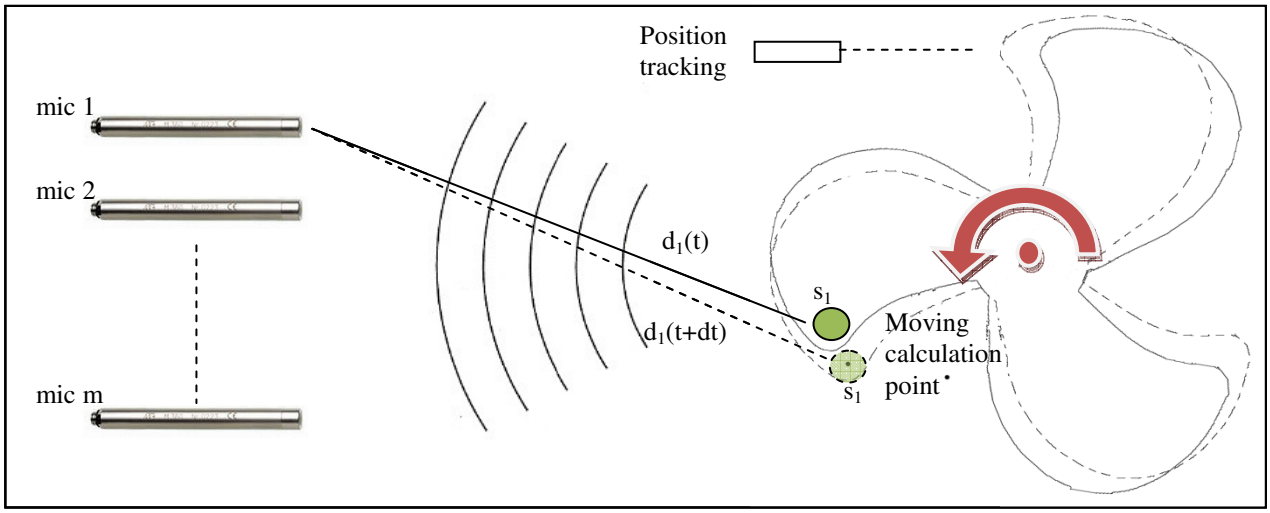

Figure 1: Near field signal delay

In the equation 1, the rotating motion will change the $\Delta_m(s)$ term with time dependency :

$$\Delta_m(s,t) = \frac{d_m(s,t)}{c} \tag{2}$$

with $\Delta_m(s,t)$ the time delay between calculation point s and at date t, $d_m(s,t)$ the distance between source s, microphone m at the date t, and c the speed of sound.

Equation 1 becomes :

$$P(s,t) = \sum_{m=1}^{M} w_m(t) \times P_m(t + \frac{d_m(s,t)}{c}) \tag{3}$$

with $w_m(t)$ the weighting applied on microphones proportional to the distance.

This formulation has the advantage to take into account the time delays, and the Doppler effect due to the rotation of the source. This algorithm is suitable for general moving objet like pass by applications.

Data re-sampling

From equation 3, the signal reconstructed at source location will lead to irregular sampled temporal signal on microphone. The best way to re-sample signal with good results is to interpolate linearly data, and to use a sampling frequency more than twice the analysis frequency.

Autospectra exclusion

Equation 3 can be re-written as :

$$P(s,t) = \sum_{m=1}^{M} A_m(s,t) \tag{4}$$

with $A_m(s,t) = w_m(t) \times P_m(t + \frac{d_m(s,t)}{c})$

In practical implementation, before summation over microphone is achieved, the temporal signal is shift to frequency domain. Moreover, the autospectra terms are removed from the summation in order to cancel microphone self noise which can be electric noise or some real noise like wind noise on the microphone itself. Finally, we compute:

$$P^2(s,f) = \sum_{n \neq m}^{M} 2A_m^*(f) \times A_n(f) \qquad (5)$$

VALIDATION FOR BOTH MOVING AND STATIONNARY NOISE

Tonal source

First validation has been done for a tonal source at 3000Hz. This source consists in a small speaker plugged on a signal generator. It is fixed on a motor with a speed of 1000 rpm

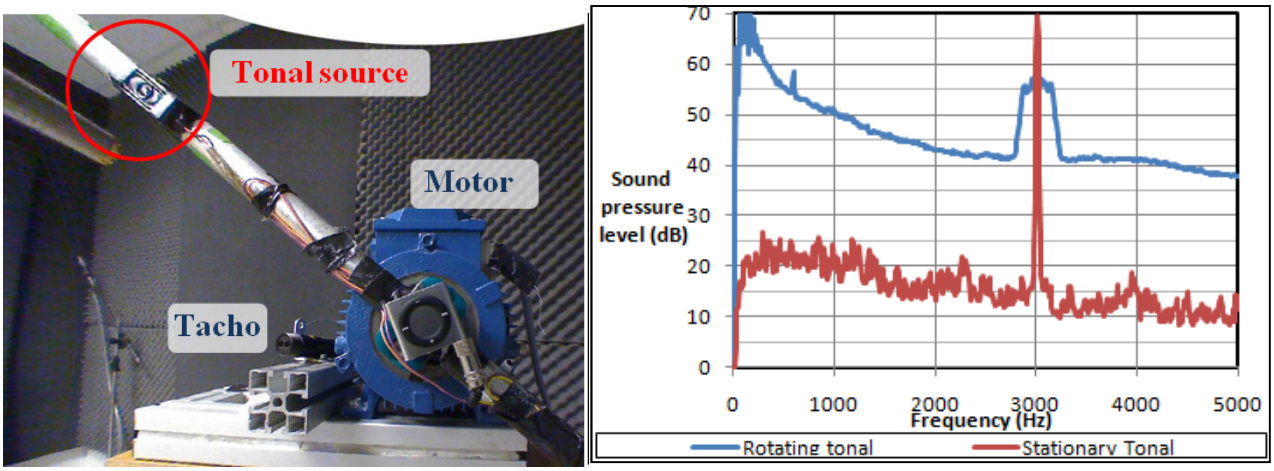

Figure 2: Tonal source test setup (left); typical pressure spectrum for rotating and stationary source (right)

In Figure 2, the typical spectrum recorded in front of the source is given. When rotating, a frequency shift due to Doppler effect is clearly visible. In terms of level, it is visible that if the rotating sources are treated with the wrong algorithm, its level is underestimated. Fixed and rotating measurements have been performed for the same source with the same level. Figure 3 shows the spectrum back-propagated on the source. The reconstructed level for rotating source shows that the frequency of the source is now correctly estimated. Both levels computed with rotating processing and fixed processing are equivalent at 3000 Hz. It shows the capability of the algorithm to estimate correctly the sound pressure level.

Outside the sound source frequency, the global spectrum has more level due to the aerodynamic noise emitted by the system itself (motor and rotating axis).

In addition, the figure 3 present the spectrum of the rotating tonal source treated with the stationary algorithm. It appears that the level over the whole frequency band is lower with the stationary algorithm than with the rotating algorithm. It thus makes it possible by comparing the level given by the two algorithms to understand if the sound source is rotating or fixed.

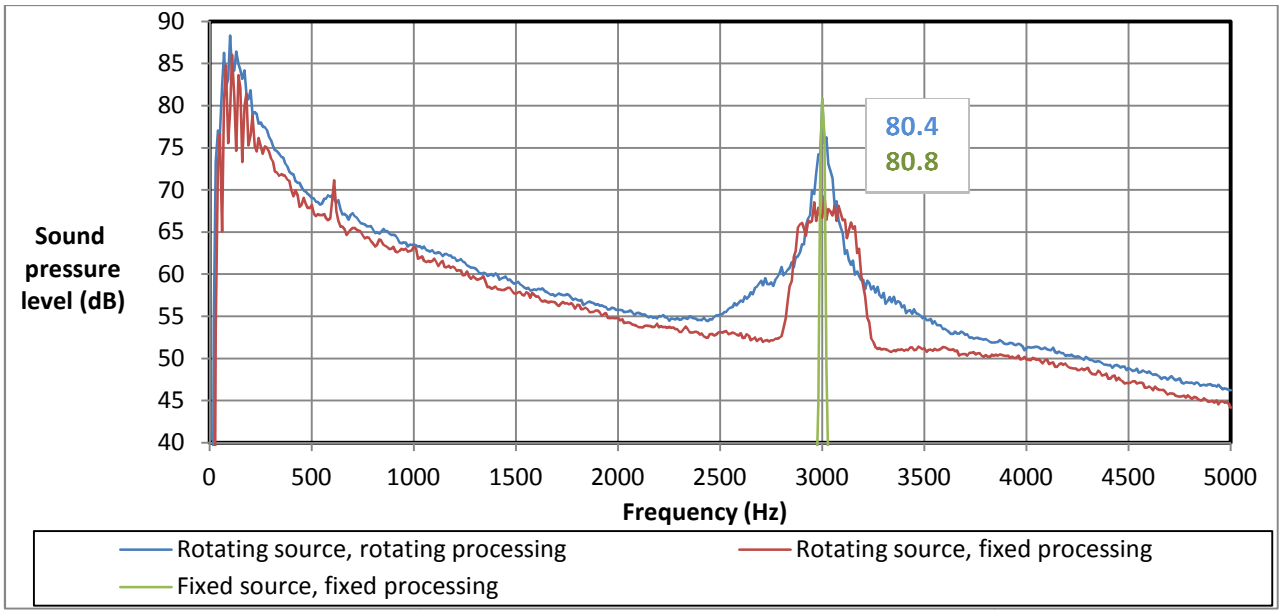

Figure 3: Sound pressure estimation at the source location

Broadband rotating source with stationary tonal

In real fan noise applications, tonal noise often radiates from the fixed parts of the fan (counter blades, fixing elements). To be more close to this case, a second experiment has been performed. It consists in two broadband noises fixed on the rotating axis, and two other tonal sources which will be stationary (figure 4). The goal of this approach is to show capability of the algorithm to separate both rotating and fixed sources.

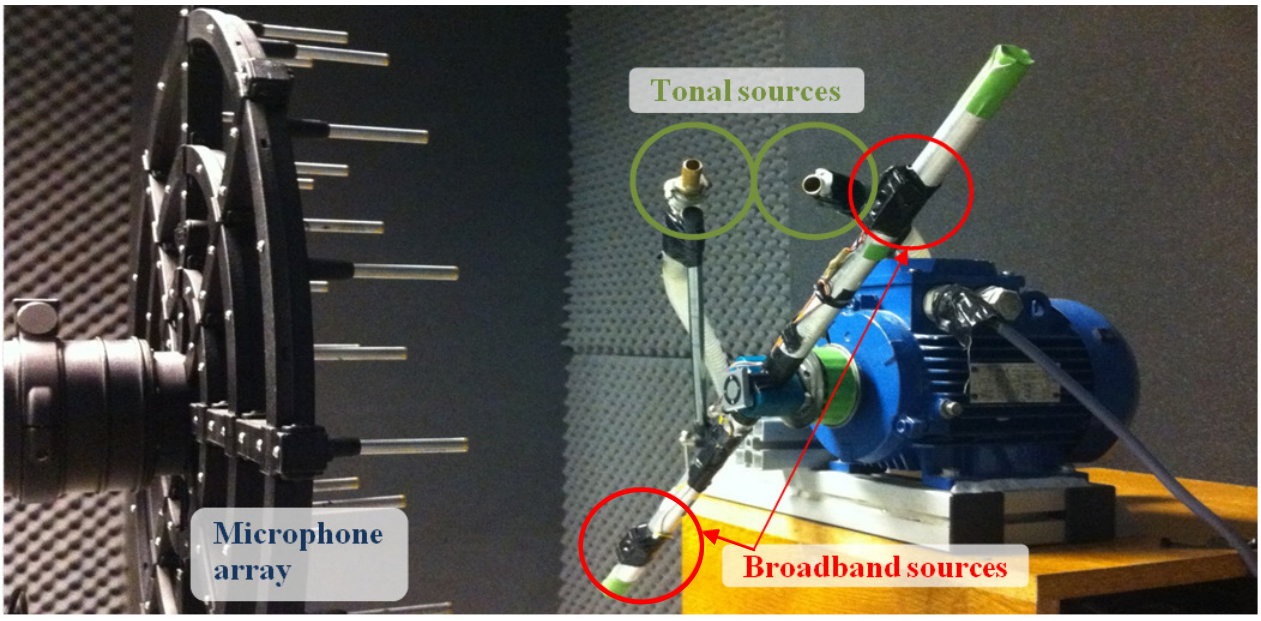

Figure 4: Test setup with fixed and rotating sound source in front of the array.

Tonal sources have been tuned to 1800 and 3000 Hz, broadband sources are fixed on the rotating axis, speed for this measurement is 1500 rpm. Figure 5 shows the average pressure level on the calculation grid.

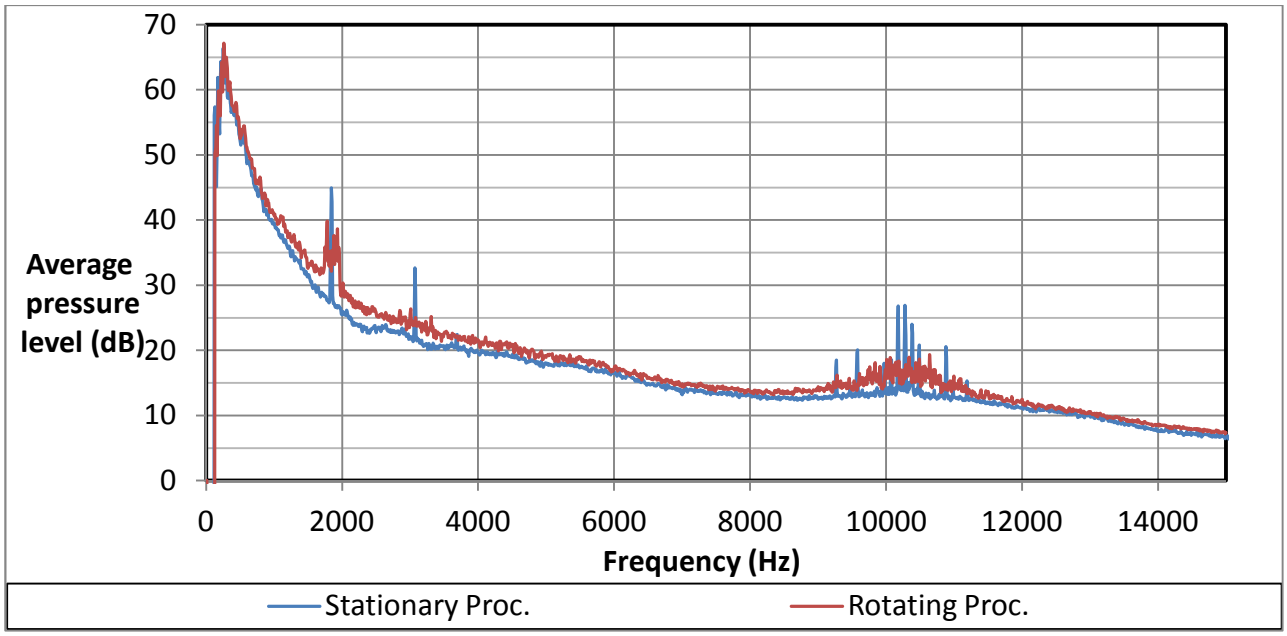

Figure 5: Average sound pressure level on the calculation grid.

As previously mentioned, by considering that the higher pressure level is given when algorithm used match real nature of sources, it appears that tonal sources are some stationary sources, and broadband noise is rotating noise. The noise around 10 kHz, comes from the electric motor itself, so it is also stationary noise.

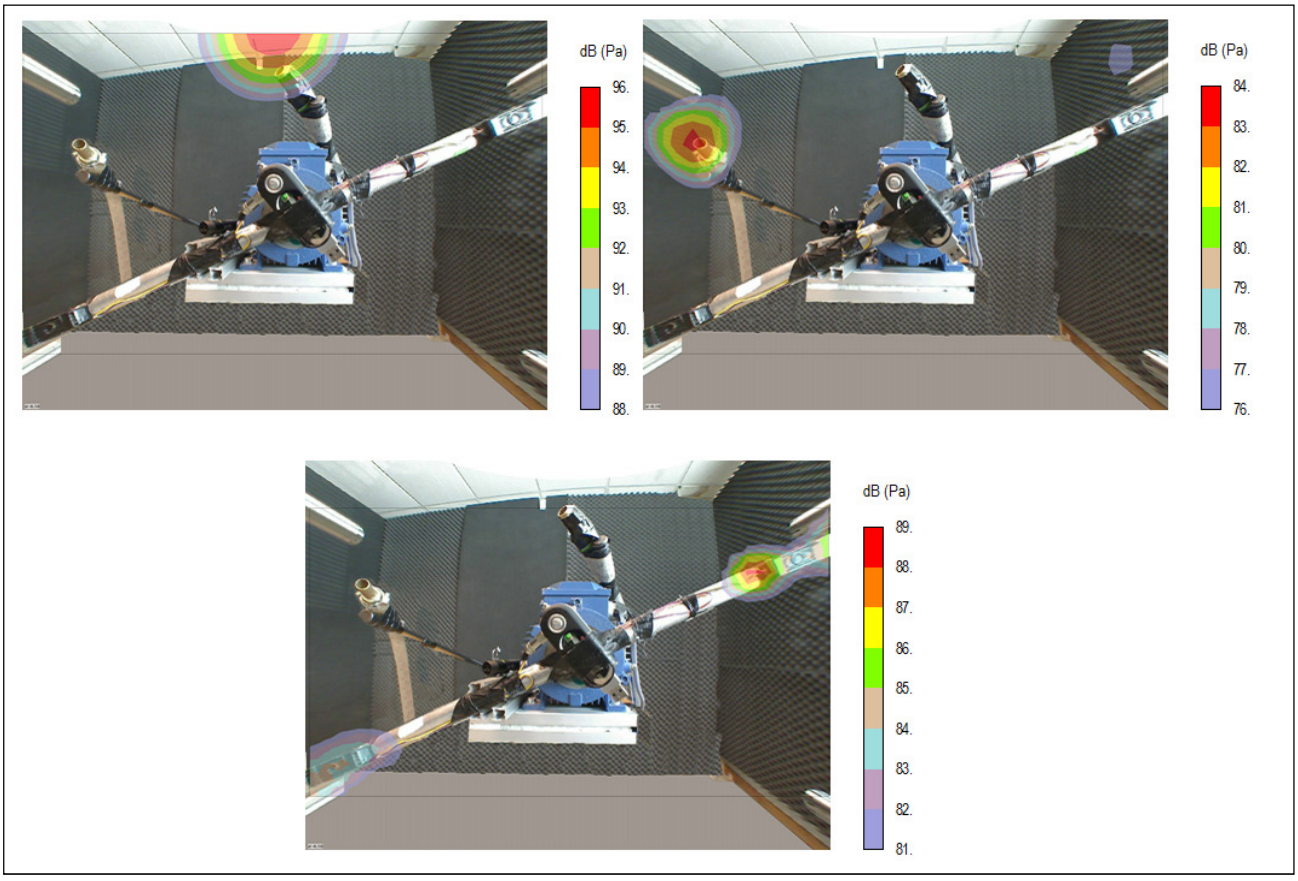

Figure 6: Acoustic hologram fixed tonal source 1800 Hz (top left), tonal 3000 Hz (top right), and rotating broadband noise (bottom).

CASE STUDY ON A FAN

Our case concerns an industrial fan used in aeronautics industry for air extraction. It consists in an axial fan with 11 blades on the rotor, and 31 blades on the stator. Rotor diameter is around 200 mm, and rotational speed around 10000 RPM. The fan is mounted inside a duct.

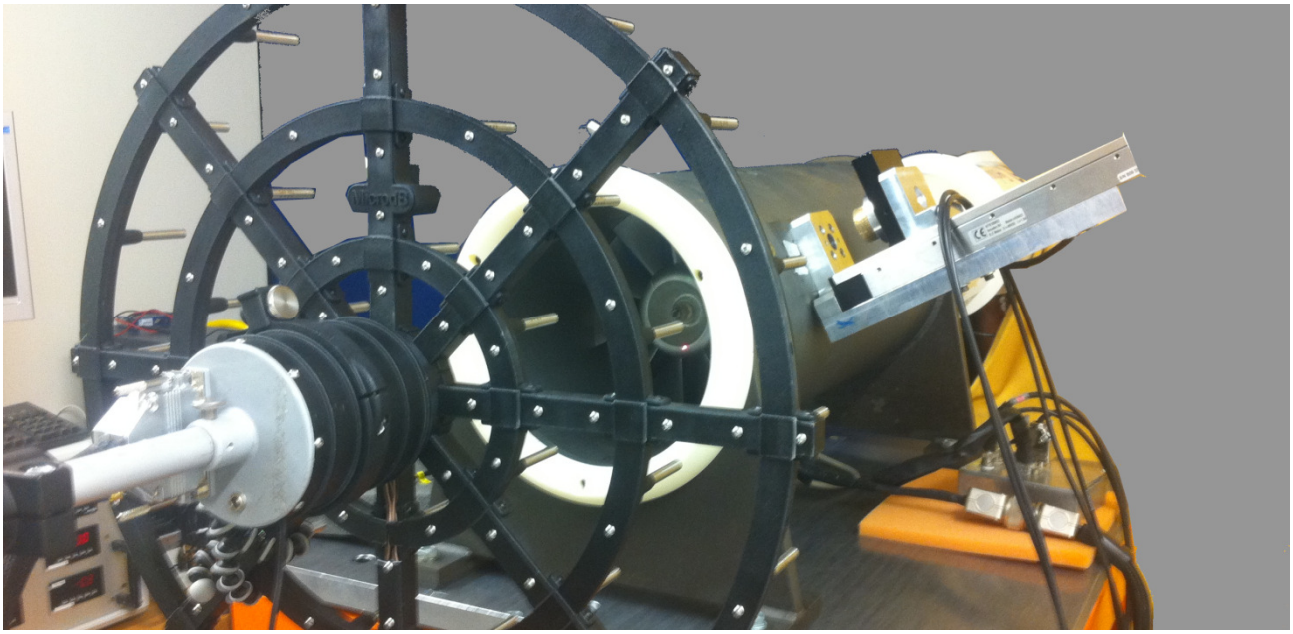

Figure 7: Test setup at the ISAE test bench.

Validation of the algorithm for high rotational speed

The goal of the first measurement is to validate the processing for a 10000 RPM rotational speed (counter clockwise). The noise is generated by two obstacles fixed on two blades, which produce a stall.

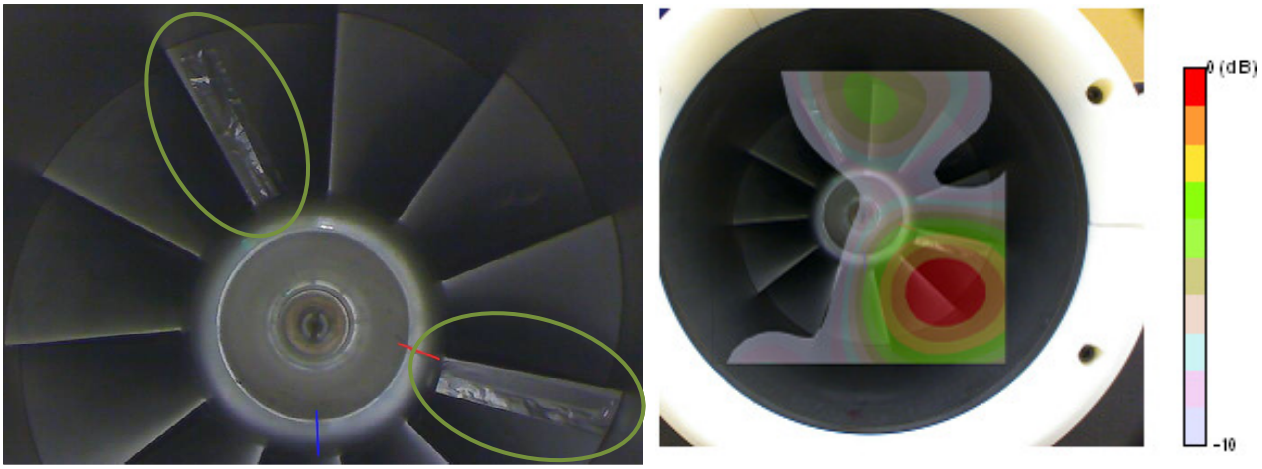

Figure 8: Obstacles on blades(left), and sound source localization (right)

Those obstacles are shown in Figure 8, they are fixed just after the leading edge of the blade. The angle between the two blades has been chosen to avoid amplifying reflection or secondary lobe of the array. Hologram is presented in Figure 8, for the two obstacles, it is clear that the source is created on the following blade at its tip area. To confirm this behavior, a second measurement at 5000 RPM has been done and gives the same localization.

Standard fan analysis

In [2] Alain Guédel gives some rules about the noise sound generation on fans. Giving these rules, we may find the blade pass frequency and its harmonics as stationary sources radiating near the stator blades, and some broadband noise as rotating source on the trailing edge

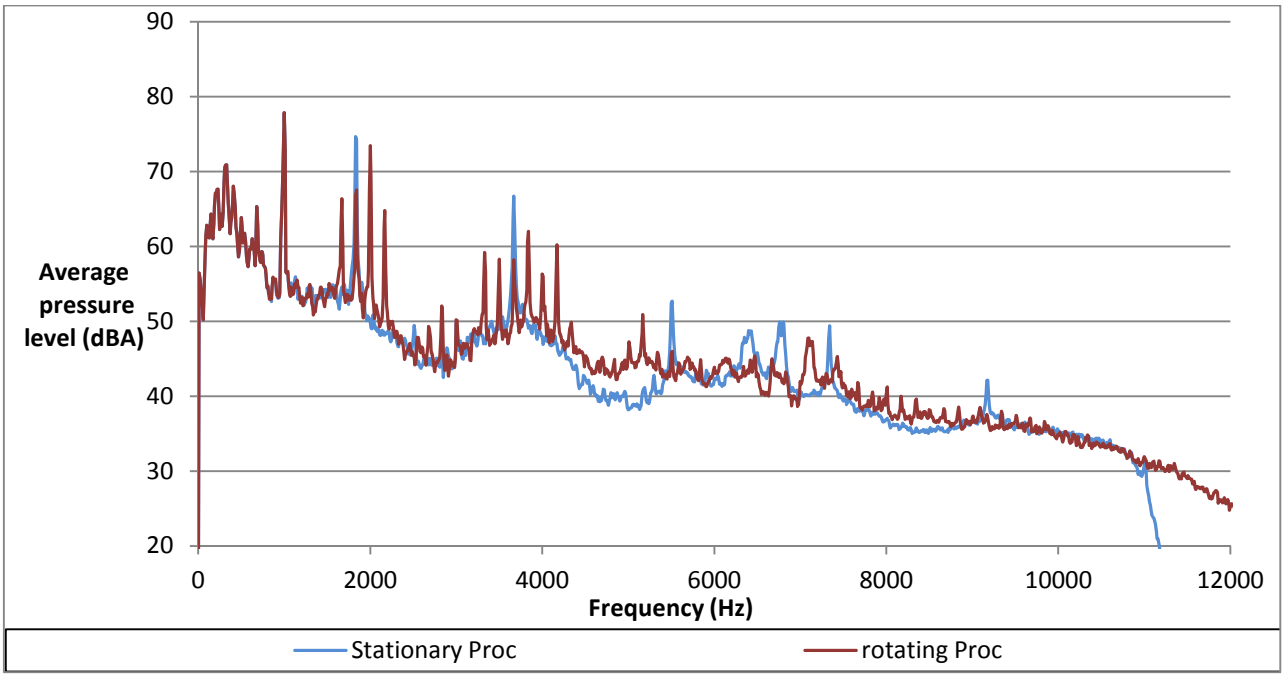

Figure 9: Pressure level on calculation grid with and without rotating processing

Figure 9 presents the spectrum for both stationary and rotating processing. Considering that the maximum level is found when used algorithm match the real nature of sources, it is possible to know if sources are rotating or not. Results are consistent with theoretical results given by Guedel. A nice improvement of this approach would be to filter stationary tonal signal on microphone before doing the rotating treatment.

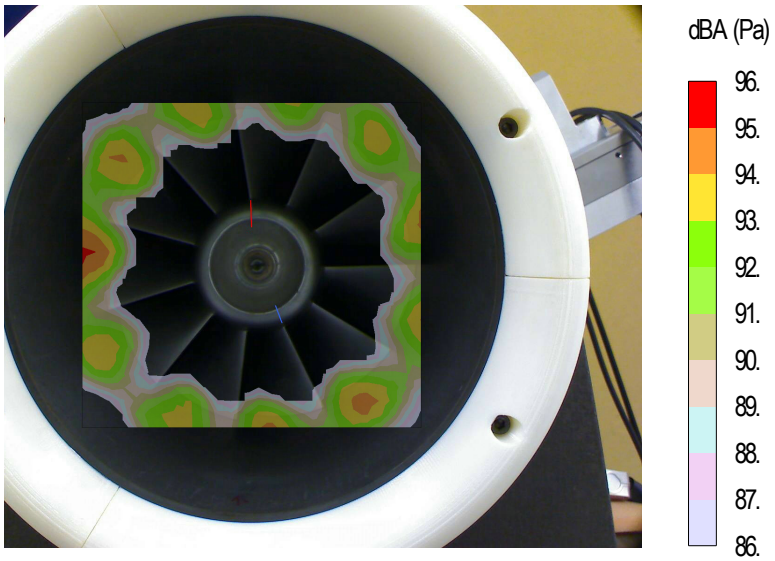

Figure 10: Hologram with rotating processing, in frequency range 4500-5500Hz

Figure 10 is the rotating processing done around 5000 Hz, it clearly shows the trailing edge of each blade.

CONCLUSION

The article presents an algorithm to analyze rotating sources and to separate stationary of rotating ones. The test case on a "in duct fan", has shown its capability to correctly track a high speed fan. For further analysis on such device, Green functions (in free field condition in our application) have to be estimated closer to the real environment.

BIBLIOGRAPHY

[1] P. Sijtsma, S. Oerlemans, H. Holthusen – *Location of rotating sources by phased array measurements*, 7th AIAA/CEAS Aeroacoustics Conference, Maastricht, **2001**

[2] A. Guédel – *Acoustique des ventilateurs - Génération du bruit et moyen de réduction*. Editions PYC LIVRES, **1999**